

Multiscale model for atomic force microscope array mechanical behavior

M. Lenczner^{a)}

Laboratoire M3M, Université Technologique de Belfort-Montbéliard, 90010 Belfort, Cedex, France

(Received 2 December 2006; accepted 26 January 2007; published online 27 February 2007)

The author presents a first simplified two-scale model of the elastic structure of an atomic force microscope array. It can be used for rapid prototyping and for designing model based control loops. Its derivation is based on the concept of two-scale approximation. © 2007 American Institute of Physics. [DOI: 10.1063/1.2710001]

The atomic force microscopy (AFM) has been invented by Binnig and reported in Ref. 1. Since that time, many applications have emerged in various fields of sciences and technologies. The main limitations of the AFM devices are their low speed and reliability of operation. This may be improved by designing model based control, see, for instance, Ref. 2. Today, the technology has evolved towards fabrication of AFM arrays, see, e.g., Ref. 3, and model based control can also help to improve their efficiency. In this letter we present, for the first time, a simplified elastic AFM array model that can be used for control as well as for rapid prototyping. Its rigorous derivation is based on the mathematical concept of two-scale approximation, see Refs. 4–6, and will be reported in a forthcoming paper.

We consider a two-dimensional array of AFMs comprised of n_2 parallel elastic bases, oriented in the x_1 direction, and n_1 clamped elastic cantilevers per base. The cantilevers are equipped with a rigid tip. They are oriented in the x_2 direction and are distributed periodically along the bases, see Fig. 1. The characteristic size of a periodicity cell is denoted by ε . The length, the width, and the thickness of the bases are denoted by L_B , $\varepsilon\ell_B$, and a_B . Those of the supple part and of the rigid part of the cantilevers are, respectively, εL_F , $\varepsilon\ell_F$, a_F and $\varepsilon L_{\text{tip}}$, $\varepsilon\ell_{\text{tip}} = \varepsilon\ell_F$, a_{tip} , see Fig. 2 for the in-plane dimensions. The array is comprised of an isotropic homogeneous material with density ρ and Lamé constants λ and μ . It occupies the domain denoted by Ω_P and is assumed to be thin enough for being modeled by the Love-Kirchhoff thin plate equation. For the sake of shortness, we consider only forces applied to the cantilever tips.

The domain Ω_P is included in $\Omega = \omega \times (-\ell_3\varepsilon/2, \ell_3\varepsilon/2)$ with section $\omega = (0, L_1) \times (0, L_2)$ and decomposed in a set of $n_1 \times n_2$ cells of periodicity Y_i with size $\varepsilon\ell_1 \times \varepsilon\ell_2 \times \varepsilon\ell_3$. In other words, $L_1 = n_1\ell_1$, $L_2 = n_2\ell_2$, and the multi-index $i = (i_1, i_2)$ varies in $\{1, \dots, n_1\} \times \{1, \dots, n_2\}$. We introduce the reference cell $Y = \prod_{j=1}^3 (-\ell_j/2, \ell_j/2)$ deduced from the cells Y_i by a shift and a dilatation by $1/\varepsilon$. Through the same shifts and dilatation, the intersections $Y_i \cap \Omega_P$ are transformed into the array reference cell $Y_P \subset Y$.

We denote by $u^P(t, x)$ the transverse mechanical displacement solution of the Love-Kirchhoff thin plate equation in Ω_P which is independent of x_3 . Its two-scale approximation is defined through the three following steps where the time variable plays the role of a parameter.

- (1) The two-scale transform \hat{u}^P of u^P is a function of the variable macro $\tilde{x} \in \omega$ and of the variable micro $y \in Y_P$. It is defined by

$$\hat{u}^P(t, \tilde{x}, y) = \sum_{i \in \{1, \dots, n_1\} \times \{1, \dots, n_2\}} \chi_{Y_i}(\tilde{x}, 0) u^P(t, x_i + \varepsilon y),$$

x_i denoting the center of Y_i .

- (2) The AFM size $L_1 \times L_2$ being frozen, we consider the geometry of the array as depending on the parameter ε . Thus, the two-scale transform \hat{u}^P is a function of ε which is assumed to be sufficiently regular so that the expansion

$$\hat{u}^P = u^A + O(\varepsilon)$$

holds, with u^A a function defined on $\omega \times Y_P$ independent of ε .

- (3) Finally, the two-scale approximation of u^P is \bar{u}^A defined on Ω_P by

$$\bar{u}^A(t, \tilde{x}) = \sum_{i \in \{1, \dots, n_1\} \times \{1, \dots, n_2\}} \chi_{Y_i}(\tilde{x}, 0) u^A(t, x_1, (x_2 - x_{i2})/\varepsilon)$$

for a function u^A depending on (t, x_1, y_2) only.

Now, we state the AFM array model, for one row, under the assumption that the displacement in each cantilever is constant in the x_1 direction and that the cantilevers are much thinner than the base or more precisely that $a_F/a_B \approx (\varepsilon/L_1)^{4/3}$. Since the array is not connected in the direction x_2 , this variable plays the role of a parameter and can be ignored in the considered case. The forces applied to the tip of the i th cell are denoted by F_i . For the sake of convenience, let us introduce the variable $y_2^C = y_2 - \ell_B + \ell_2/2$ that vanishes at the junction between the base and the cantilever in Y_P . It appears that u^A is independent of y_2 in the base, so the model equations are expressed in the rectangular domain $(x_1, y_2^C) \in (0, L_1) \times [0, L_F + L_{\text{tip}})$. The line $y_2^C = 0$ corresponds to the base, the open rectangle $(0, L_1) \times (0, L_F)$ represents the elastic part of the cantilevers, and $(0, L_1) \times (L_F, L_F + L_{\text{tip}})$ its rigid part. For $t > 0$ and $x_1 \in (0, L_1)$,

$$\rho^M \partial_t^2 u^A + R^M \partial_{x_1 \dots x_1}^A u^A + \ell_R R^C \partial_{y_2 y_2}^C u^A = 0 \quad (1)$$

for $y_2^C = 0$ and

$$\rho^F \partial_t^2 u^A + R^C \partial_{y_2 \dots y_2}^A u^A = 0 \quad (2)$$

for $y_2^C \in (0, L_F)$. The boundary conditions are $u^A = \partial_{x_1} u^A = 0$ for $(x_1, y_2^C) \in \{0, L_1\} \times \{0\}$, $\partial_{y_2} u^A = 0$ for $(x_1, y_2^C) \in (0, L_1) \times \{0\}$, and

^{a)}Electronic mail: michel.lenczner@utbm.fr

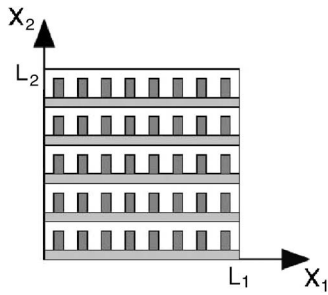


FIG. 1. Array of cantilevers.

$$\begin{aligned} \rho^R \partial_{t1}^2 \begin{pmatrix} u^A \\ \partial_{y_2} u^A \end{pmatrix} + \ell_F R^C Q \begin{pmatrix} -\partial_{y_2 \dots y_2}^3 u^A \\ \partial_{y_2 y_2}^2 u^A \end{pmatrix} \\ = \frac{1}{\varepsilon} M(y_2^{C_{tip}}) \sum_i F_i \delta_{(x_1)_i}(x_1) \end{aligned}$$

for $(x_1, y_2^C) \in (0, L_1) \times \{L_F\}$, where the sum holds on the cells belonging to the row of cantilevers and where $y_2^{C_{tip}}$ is the second coordinate of the tip in Y_p . Once u^A is computed in the elastic part, its expression in the rigid part is

$$u^A = M(y_2^C) \begin{pmatrix} u^A(L_F) \\ \partial_{y_2} u^A(L_F) \end{pmatrix}.$$

The initial conditions are on u^A and on $\partial_t u^A$ in $(0, L_1) \times [0, L_F)$. Let us denote by Y_R the rigid part in the reference cell Y and by y_{G2}^C the coordinate y_2^C of the mass center. The parameters of the model are $Q^F = (\varepsilon/2a_F L_F^4 \ell_F) Q$, $N(y_2^C) = \begin{pmatrix} 1 & y_2^C \\ 0 & 1 \end{pmatrix}$, $M(y_2^C) = (1, 0) N(y_2^C) N^{-1}(L_F)$, $J_0^A = |Y_R|$, $J_2^A = \int_{Y_R} (y_2^C - y_{G2}^C)^2 dy_2^C$, $L_{F,G} = L_F - y_{G2}^C$, $Q = J_0^A \begin{pmatrix} 1 & -L_{F,G} \\ -L_{F,G} & J_2^A / J_0^A + L_{F,G}^2 \end{pmatrix}$, $\rho^M = 2a_B \ell_B \rho$, $\rho^F = 2a_F \rho$, $\rho^R = \varepsilon \rho$, $R^M = [4\ell_B a_B^3 \mu / 3(\lambda + 2\mu)] \times (2(\lambda + \mu) - \lambda^2 / 2(\lambda + \mu))$, and $R^C = 8\varepsilon^4 a_F^3 \mu (\lambda + \mu) / 3(\lambda + 2\mu)$.

Remark: If the cantilevers are not equipped with a rigid part, the model must be modified by setting $Q=0$.

For the model illustration, some simulations with a force oscillating at the first cantilever eigenfrequency and applied to the fifth tip (a) or to the fifth and sixth tips (b) have been conducted. The structure is isotropic and homogeneous, its volume mass is $\rho = 2329 \text{ kg/m}^3$, and its Lamé coeff cients are $\lambda = 6.1 \times 10^{11}$ and $\mu = 5.2 \times 10^{11}$. The other parameters are $\varepsilon = 50 \text{ }\mu\text{m}$, $\ell_1 = 1$, $n_1 = 10$, $n_2 = 1$, $\ell_B = 0.333$, $a_B = \varepsilon/5 \text{ m}$,

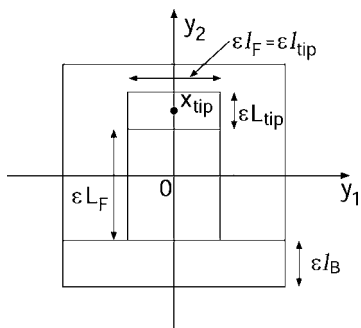


FIG. 2. Two-dimensional cell.

TABLE I. Ratios of the maximum displacement of the ten tips to these of the excited tips: (a) the fifth tip and (b) the fifth and the sixth tips.

Tips	1	2	3	4	5	6	7	8	9	10
(a) (%)	8	9	11	12	100	13	12	11	1	0.9
(b) (%)	1.2	0.5	0.3	0.2	100	100	0.2	0.3	0.5	1.2

$\ell_F = \ell_{tip} = L_{tip} = 0.25$, $L_F = 0.833$, $a_F = \varepsilon/40 \text{ m}$, and $a_{tip} = \varepsilon/2 \text{ m}$. The ratios of the maximum displacement of the ten tips to these of the excited tips [(a) the fifth tip and (b) the fifth and the sixth tips] are reported in Table I.

We denote by (λ^A, ψ^A) the solutions of the associated spectral problem which is derived from the above model by replacing u^A by ψ^A and ∂_{tt}^2 by $-\lambda^A$. They constitutes an infinite sequence and can be written under the form $\lambda_{k_1 k_2}^A = R^C \lambda_{k_1 k_2}^C / (\rho^F L_F^4)$ and $\psi_{k_1 k_2}^A(x_1, y_2) = \varphi_{k_1}^B(x_1/L_1) \varphi_{k_2}^C(y_2/L_F)$ for $(k_1, k_2) \in \mathbb{N}^* \times \mathbb{N}$, where $(\lambda_{k_1}^B, \varphi_{k_1}^B)$ is the solution of the spectral problem

$$\varphi^{B''''} = \lambda^B \varphi^B \quad \text{in } (0, 1),$$

$$\varphi^B = \varphi^{B'} = 0 \quad \text{at } \{0, 1\},$$

and for each λ^B , (λ^C, φ^C) is the solution of the spectral problem

$$\varphi^{C''''} = \lambda^C \varphi^C \quad \text{in } (0, 1),$$

$$\varphi^{C'}(0) = 0,$$

$$\begin{pmatrix} -\varphi^{C''}(1) \\ \varphi^{C''}(1) \end{pmatrix} = \lambda^C Q^A \begin{pmatrix} \varphi^C(1) \\ \varphi^{C'}(1) \end{pmatrix}, \quad (3)$$

and

$$q^1 \varphi^{C''}(0) = (q^0 \lambda^C - \lambda^B) \varphi^C(0),$$

with $Q^A = (\varepsilon/2a_F L_F \ell_F) S Q S$, $S = \begin{pmatrix} 1 & 0 \\ 0 & 1/L_F \end{pmatrix}$, $q^0 = L^4 R^C \rho^M / (L_F^4 R^M \rho^F)$, and $q^1 = L^4 R^C \ell_F / (L_F^3 R^M)$. For λ^B large enough, (λ^C, φ^C) are independent of λ^B , so they may be indexed by the index k_2 only. In our simulations, we have

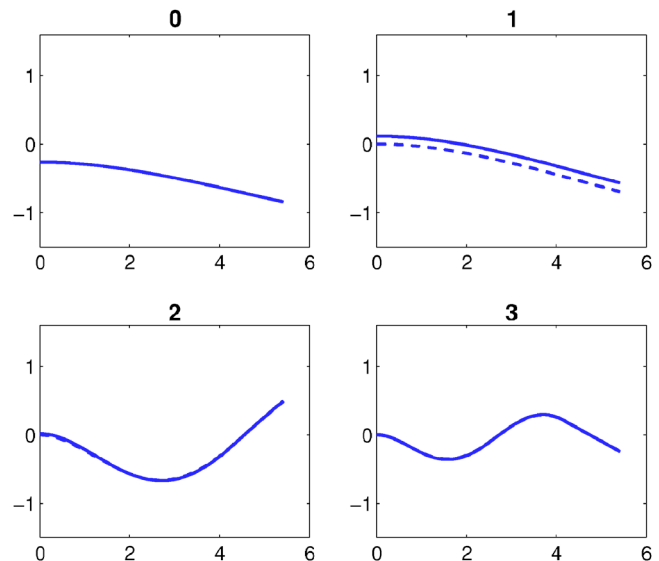


FIG. 3. Shapes of $(\varphi_{k_2}^C)_{k_2=0, \dots, 3}$ in solid line superimposed on $(\varphi_{k_2}^B)_{k_2=1, \dots, 3}$ in dashed line.

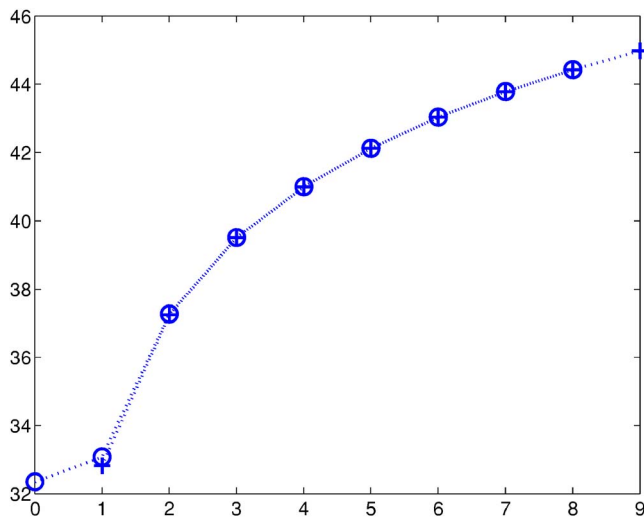


FIG. 4. Logarithm of the eigenvalues $(\lambda_{k_2}^P)_{k_2=1,\dots,9}$ (o) and $(\lambda_{k_2}^C)_{k_2=0,\dots,8}$ (+).

found that this was always the case. We denote by (λ^P, φ^P) the solution of the spectral problem associated with a single clamped cantilever. It is governed by the same equation that Eq. (3), except that the last boundary condition is replaced by $\varphi^P(0)=0$. The first graph of Fig. 3 represents the eigenvector φ_0^C and the others the superimposed images of the eigenvectors $\varphi_{k_2}^C$ in solid line and of the eigenvectors $\varphi_{k_2}^P$ in dashed line for $k_2=1, \dots, 3$. For $k_2 \geq 1$, the modes $\varphi_{k_2}^C$ and $\varphi_{k_2}^P$ differ mainly by a constant that becomes smaller when k_2 increases. The logarithm of the eigenvalues $\lambda_{k_2}^A$ for

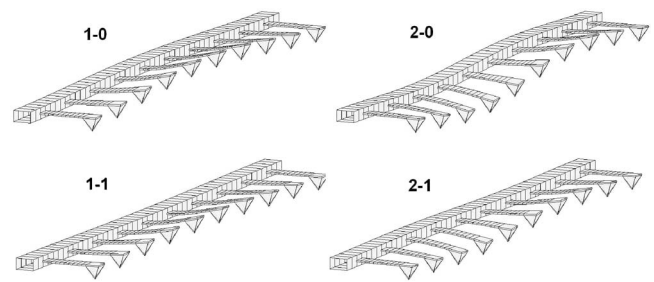


FIG. 5. Array modes $\psi_{(k_1,k_2)}^A$ for $k_1=1, 2$ and $k_2=0, 1$.

$k_2=0, \dots, 8$ with markers “o” and $\lambda_{k_2}^P$ for $k_2=1, \dots, 9$ with markers “+” is compared in Fig. 4. Finally, the eigenvectors ψ_{k_1,k_2}^A for $(k_1, k_2) \in \{1, 2\} \times \{0, 1\}$ are displayed in Fig. 5.

The AFM array model presented here is extremely light, so it can be used for real time model based control of the array as well as for model based image processing. Further extensions of the models are also suitable to encompass electrostatic and thermal couplings.

¹G. Binnig, C. Quate, and C. Gerber, Phys. Rev. Lett. **56**, 930 (1986).
²S. M. Salapaka, T. De, and A. Sebastian, Mech. Struct. Mach. **15**, 821 (2005).
³M. Despont, J. Brugger, U. Drechsler, U. Durig, W. Haberle, M. Lutwyche, H. Rothuizen, R. Stutz, R. Widmer, G. Binnig, H. Rohrer, and P. Vettiger, Sens. Actuators, A **80**, 100 (2000).
⁴M. Lenczner, C. R. Acad. Sci. Paris Sér. II b **324**, 537 (1997).
⁵M. Lenczner and D. Mercier, Multiscale Model. Simul. **2**, 359 (2004).
⁶D. Cioranescu, A. Damlamian, and G. Griso, C. R. Math. Acad. Sci. **335**, 99 (2002).